Rare Metal Materials and Engineering
Volume 50, Issue 10, October 2021
Available online at www.rmme.ac.cn

Science Press

Cite this article as: Tian Chenggang, Tao Xipeng, Xu Ling, et al. Effects of Stacking Fault Energy and Temperature on Creep Performance of Ni-based Alloy with Different Co Contents[J]. Rare Metal Materials and Engineering, 2021, 50(10): 3532-3537.

ARTICLE

Effects of Stacking Fault Energy and Temperature on Creep Performance of Ni-based Alloy with Different Co Contents

Tian Chenggang[1], Tao Xipeng[2,3], Xu Ling[2], Cui Chuanyong[2], Sun Xiaofeng[2]

[1] AECC Commercial Aircraft Engine Co., Ltd, Shanghai 200241, China; [2] Superalloys Division, Institute of Metal Research, Chinese Academy of Sciences, Shenyang 110016, China; [3] School of Materials Science and Engineering, University of Science and Technology of China, Shenyang 110016, China

Abstract: The deformation microstructures of two Ni-based superalloys with different Co contents after creep tests at 650 °C/630 MPa, 725 °C/630 MPa and 760 °C/630 MPa were investigated by transmission electron microscopy (TEM), in order to study the influence of temperature and stacking fault energy (SFE) on the creep deformation mechanisms. The results show that the improvement in temperature enhances the creep mechanism transition from stacking faults to micro-twinning for the experimental single crystal alloys, suggesting that the formation of micro-twins is dependent on temperature. Moreover, increasing Co content as well as lowering SFE allow stacking faults or micro-twins to extend through the γ matrix and γ' precipitates, which improve the creep resistance and prolong the creep life of the alloys.

Key words: superalloys; stacking faults; stacking fault energy; micro-twins

Ni-based superalloys have been extensively used as turbine blades and discs in aircraft engines and industrial gas engines for their excellent high temperature mechanical properties, such as good tensile properties, low cyclic fatigue and creep properties[1-3]. In modern advanced engines, the creep resistance of the disc superalloys at elevated temperatures has become a major concern for the researchers and engineers. In Ni-based disk superalloys, the interaction between γ' precipitates and mobile dislocations plays an important role in maintaining high temperature creep properties[4]. Dislocation bypassing γ' precipitates via Orowan loop, cooperative climbing, and dislocation shearing γ' precipitates are considered as three main processes during creep deformation depending on microstructure, temperature and loading stress[4]. In the service temperature ranging from 600~800 °C for some new disk superalloys, stacking faults and deformation micro-twins due to dislocation shearing may occur[4]. However, the influence of temperature on the creep deformation for Ni-based disc superalloys is still unclear. Recently, Yuan et al[5-7] found that creep life of TMW-4M3 alloy maintains about six times larger than that of commercial U720Li alloy at 725 °C/630 MPa. Furthermore, it was suggested that the TMW-4M3 alloy exhibits low SFE due to the high Co content, facilitating the deformed micro-twinning process, which improves the creep resistance compared to U720Li alloy under the same creep condition. Tian et al[8] also found that the lower SFE due to Co addition can promote the main creep mode transition from isolated stacking fault to extended fault, and then to micro-twinning in Ni-based superalloys at 725 °C/630 MPa. However, the influence of SFE on creep deformation mechanisms of Ni-based superalloys was mainly focused on the case under the condiftion of 725 °C and 630 MPa in previous studies. Understanding the deformation behavior affected by SFE in a wide temperature range will be helpful for designing new disk alloys. Therefore, two Ni-based superalloys with different Co contents were evaluated by creep tests at temperatures of 650~760 °C under a stress of 630 MPa in order to systematically study the effects of temperature and SFE on creep deformation mechanisms.

1 Experiment

The nominal composition of two Ni-based disc superalloys

Received date: October 13, 2020
Foundation item: High Technology Research and Development Program of China (N2014AA041701); National Natural Science Foundation of China (51171179, 51271174, 51331005, 11332010)
Corresponding author: Tian Chenggang, Ph. D., AECC Commercial Aircraft Engine Co., Ltd, Shanghai 200241, P. R. China, E-mail: 562286459@qq.com

for creep tests is listed in Table 1. The alloys are named as U1 and U2. For the test alloys, 20 kg ingots were cast using the vacuum induction melting (VIM) method. These ingots were then hot extruded into bars with a diameter of 19 mm at about 1160 °C. The extrusion bars were heat treated under 1170 °C/4 h/air cooling (AC)+1080 °C/4 h/AC followed by aging under 845 °C/24 h/AC+760 °C/16 h/AC. The specimens for creep tests with a gauge length of 25 mm and a diameter of 5 mm were cut from the heat treated bars. Constant-load tensile creep tests were operated at various temperatures and loading stresses. The temperatures are listed as follows: 650 °C (T_1)< 725 °C (T_2)<760 °C (T_3), and the loading stress is 630 MPa (σ). For microstructure characterization, the samples for optical microscopy (OM) observation were etched in a solution of Kalling reagent. The samples for scanning electron microscopy (SEM) observation were electronically etched in a solution of 17 mL H_2O +1 mL glacial acetic acid+2 mL nitric acid at 1.5 V for ~30 s. Transmission electron microscopy (TEM) discs with a thickness of ~300 μm were cut from the samples perpendicular to the stress axis. Subsequently, the discs were manually ground down to 50 μm and thinned by a twin-jet electro-polisher in a solution of 10% perchloric acid and 90% ethanol at about 16 V and -20 ℃. TEM observations were performed on a JEOL 2100 TEM operated at 200 kV.

Table 1 Nominal chemical composition of two Ni-based superalloys (wt%)

Alloy	Co	Al	Ti	Mo	Cr	C	Fe	Zr	Ni
U1	13.4	2.1	4.5	4.1	16.0	0.04	0.27	0.063	Bal.
U2	20.5	1.9	5.7	3.7	14.6	0.03	0.26	0.051	Bal.

2 Results and Discussion

2.1 Initial microstructure

The microstructures of the two alloys after heat treatment are shown in Fig. 1. The grain size of the two alloys is estimated to be around 200±25 μm, as shown in Fig. 1a and 1b. At a high magnification, a bimodal size distribution of γ' precipitates can be observed in the two alloys, as shown in Fig.1c and 1d. The sizes of γ' precipitates in the two alloys are in the range of 200~500 nm for the large ones and of 20~100 nm for the small ones.

2.2 Creep properties

The creep rupture life for the two experimental alloys is listed as follows: 406 h (T_1/σ), 221 h (T_2/σ) and 17 h (T_3/σ) for U1, 647 h (T_1/σ), 266 h (T_2/σ) and 32 h (T_3/σ) for U2. It is illustrated that the rupture life for both two alloys decreases with increasing the temperature and the creep life of U2 is longer than U1 under the same condition. Fig. 2 demonstrates four creep curves of two alloys at T_2/σ and T_3/σ. Another two creep curves for the experimental alloys at T_1/σ are not well tracked.

2.3 Deformation microstructure

For TEM observations, the foils were cut from the deformed area of 5~10 mm away from the fracture surface under each condition. Fig. 3 shows the creep deformation microstructures for the two alloys at T_1/σ. For U1, it is clearly observed that the discontinuous stacking faults extend along the same direction in large and small γ' precipitates at T_1/σ, as shown in Fig. 3a. At a higher magnification in Fig. 3b, many matrix dislocations are found in the γ channel. For U2 alloy,

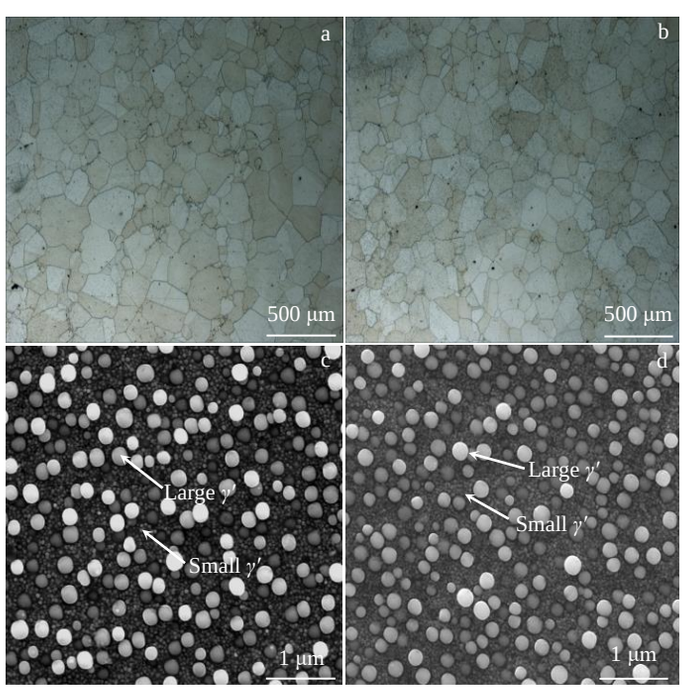

Fig.1 Microstructures for U1 (a, c) and U2 (b, d) alloys after heat-treatment: (a, b) OM images depicting the grain size and (c, d) SEM images depicting γ' precipitates distribution

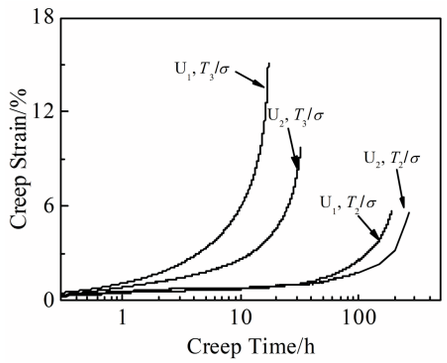

Fig.2 Creep curves for the two experimental alloys at T_2/σ and T_3/σ

however, the continuous stacking faults operated on different slip planes traverse the matrix and γ' precipitates at T_1, as shown in Fig. 3c. At the same time, Fig. 3d shows that the dissociated dislocations in the matrix are observed within the vicinity of continuous stacking faults at a high magnification.

TEM observations of the deformation microstructures at T_2/σ for the two alloys are illustrated in Fig. 4. For U1, the stacking faults and micro-twins operated on different slip planes are mainly confined in large γ' precipitates, and the density of dislocations in the γ matrix is very large, as depicted in Fig.4a. At a high magnification, it can be observed that the micro-twins are formed in small γ' precipitates in Fig. 4b. For U2, the isolated stacking fault and micro-twinning become the prominent creep modes, as shown in Fig.4c and 4d.

Fig. 5 demonstrates the creep deformation microstructures for the two alloys at T_3/σ. For U1, the isolated stacking faults and micro-twins only cut through γ' precipitates, as shown in the bright (Fig.5a) and dark (Fig.5b) field TEM images. While the bright and dark TEM images in Fig. 5c and 5d show that the dominant micro-twins extend through the γ matrix and γ' precipitates in U2 alloy.

2.4 Effects of SFE and temperature on creep mechanisms

It has been reported that Co addition tends to lower the SFE of the single crystal alloys[8-10]. As shown in Table 1, the addition content of Co in U2 is much more than that in U1, so U2 possesses a relatively lower SFE than U1. The previous studies[8, 11-13] indicated that SFE exerts significant effect on the dissociation of the matrix dislocation during deformation of Ni-based superalloys. Bobeck and Miner[13] found that lowering SFE by Co addition gives rise to the increase of the degree of dislocation dissociation in MAR-M247-based alloys. Unocic et al[12] concluded that the $a/2<110>$ matrix dislocation confined in the matrix channel will not dissociate into Shockley partial dislocation when the SFE increases from 10 mJ/m^2 to 100 mJ/m^2 through a microscopic phase field simulation. Hence the dislocation dissociation in the γ matrix is much easier in U2. The $a/2<110>$ matrix dislocation can dissociate into two Shockley partial dislocation on {111} planes by the following reaction in the γ matrix[14] :

$$\frac{\alpha}{2}<101>\longrightarrow\frac{\alpha}{6}<112>+\mathrm{SF}+\frac{\alpha}{6}<2\bar{1}1> \quad (1)$$

At T1, the dislocation dissociation reaction of Eq.(1) occurs in U2 and the dissociated Shockley partial dissociation shears the γ matrix and γ' precipitates, leaving continuous stacking faults, as shown in Fig.3c. Similar viewpoint was proposed by Decamps et al [15]. As for the formation of discontinuous stacking faults in U1, Zhang et al [16] proposed a mechanism

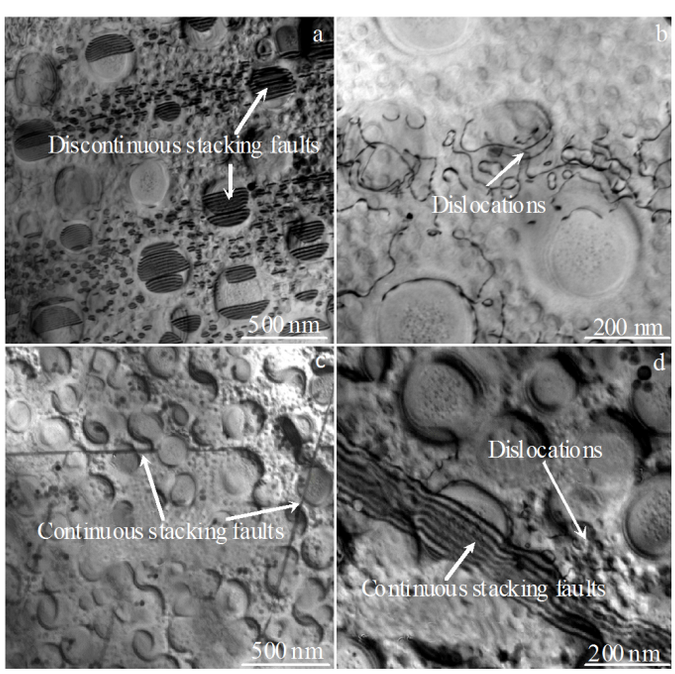

Fig.3 Microstructures after creep deformation at T_1/σ for U1 (a, b) and U2 (c, d): (a) discontinuous stacking faults, (b) matrix dislocations, (c) continuous stacking faults, and (d) dislocations within the vicinity of continuous stacking faults

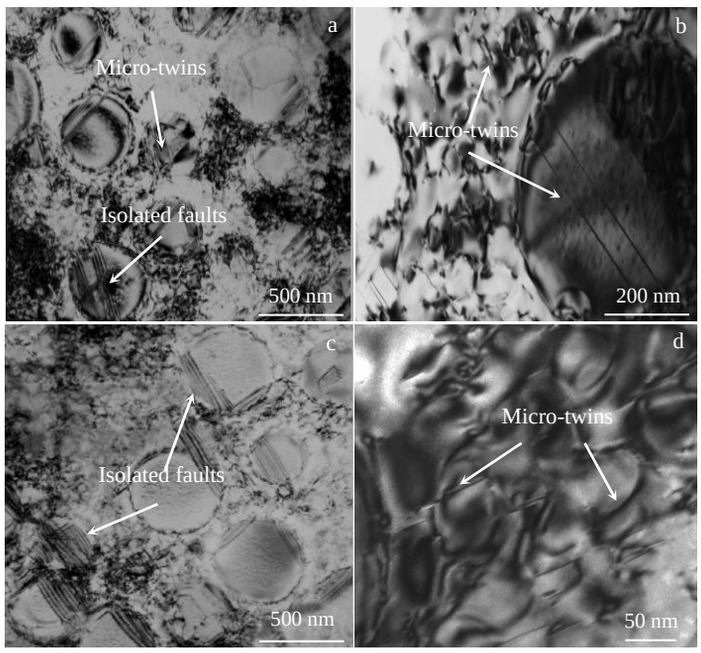

Fig.4 Microstructures after creep deformation at T_2/σ for U1 (a, b) and U2 (c, d): (a) micro-twins and isolated stacking faults shearing large γ' precipitates, (b) micro-twins shearing small γ' precipitates, (c) isolated stacking faults shearing large γ' precipitates, and (d) micro-twins shearing small γ' precipitates

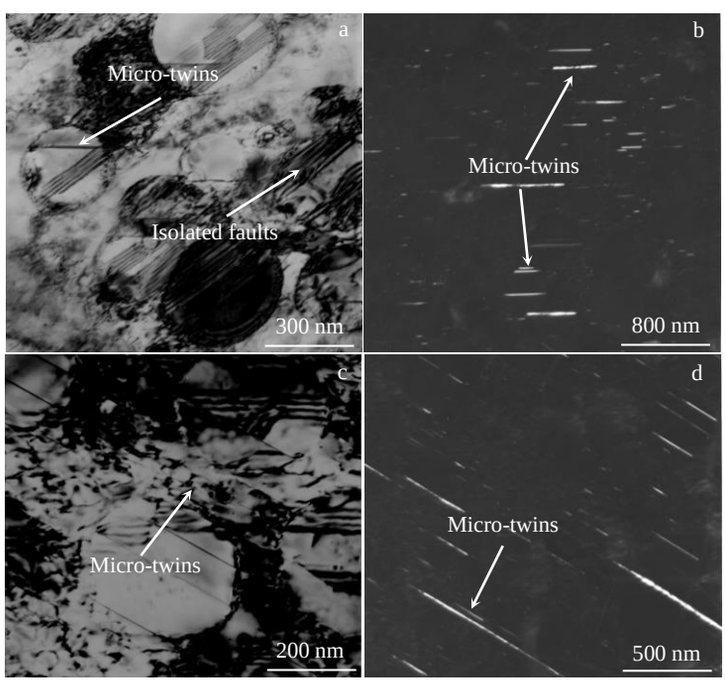

Fig.5 Bright field (a, c) and dark field (b, d) images after creep deformation at T_2/σ: (a, b) U1, micro-twins only cutting through γ' precipitates; (c, d) U2, micro-twins extending through the γ matrix and γ' precipitates

that the leading $\alpha/3[112]$ partial and the trailing $\alpha/6[211]$ partial dissociations are firstly dissociated from an interfacial $\alpha/2[011]$ dislocation, and then the $\alpha/3[112]$ partial dissociation may cut through the γ matrix and γ' precipitates, leaving the continuous extrinsic stacking faults in its wake. The $\alpha/6[211]$ partial dissociation follows the way of $\alpha/3[112]$ partial dissociation and removes the stacking faults in the γ matrix. However, this mechanism is controversial because the

shearing in the γ matrix by $\alpha/3[112]$ partial dissociation is generally not accepted. It can be deduced that the $\alpha/2<110>$ matrix dislocation does not dissociate until it reaches γ/γ' interface with the aid of the coherency stress at T_1 in U1. Subsequently, the discontinuous stacking faults in γ' precipitates are created by the shearing of the Shockley partial dissociation produced at γ/γ' interface according to Viswanathan et al [17], as shown in Fig. 3a.

At T2, the fast diffusion rate and adequate diffusion time cause stacking fault exchange between Ni and Al atoms, which leads to the formation of micro-twins in two alloys according to Koble's model [18]. In this model, the micro-twin is converted by a pseudo-twin structure as well as a two-layer complex stacking fault (CSF) through atomic reordering. Sarosi et al [19] identified that the CSF layer can only be created by the shearing of Shockley partial dissociation from TEM evidence. In addition, the atomic reordering between Al and Ni atoms in the micro-twinning process has been verified by Kovarik et al [14] via the ab initio calculations. Meanwhile, the ease of cross slips due to the operation of multiple slip systems makes the formation of continuous stacking faults (or micro-twins) quite difficult in U2 at T_2, as shown in Fig. 4c. But the dislocation dissociation in the γ matrix in U2 still exists. Besides, another dislocation dissociation scheme proposed by Caron et al[20]. may occur at γ/γ' interface of two alloys at this temperature according to the following reaction [20]:

$$\frac{\alpha}{2}<1\bar{1}0>\longrightarrow\frac{\alpha}{3}<1\bar{2}1>+\mathrm{SISF}+\frac{\alpha}{6}<11\bar{2}> \quad (2)$$

where the superlattice partial shears γ' precipitates, creating superlattice intrinsic stacking fault (SISF). Similarly, Milligan and Condat et al[21,22] proposed that SISF in γ' precipitates can be created by the shearing of $\alpha/3[112]$ partial dislocation. Thus the shearing by $\alpha/6[112]$ and $\alpha/3[112]$ partial dislocation may occur simultaneously during creep deformation for two alloys at high temperatures.

At T_3, the rupture life for the two experimental alloys decreases rapidly. However, the micro-twins can still be observed in the two alloys, as exhibited in Fig. 5a~5d, which indicates that the atomic reordering and the shearing processes may occur simultaneously during the micro-twinning process at T_3. Due to the high SFE of U1, the dislocation shearing is still mainly restricted in γ' precipitates, while the extended micro-twins due to the continuous shearing in the γ matrix and γ' precipitates are formed in U2 with low SFE. Some researchers [17] believed that the micro-twinning occurs when the creep rate is relatively low. But in this study, the micro-twins are created at a high creep rate and high temperatures, which implies that the formation of micro-twins is mainly dependent on temperature.

2.5 Thermodynamic calculation

With increasing the temperature, the creep rupture life for the two alloys sharply decreases due to the ease of cross-slips and fiercer shearing. Additionally, the isolated stacking faults and micro-twins created in γ' precipitates cannot interact with mobile dislocations in the γ matrix in U1 alloy. Moreover, the shearing in γ' precipitates might help to relieve strain hardening and promote dislocation movements in the γ matrix. While high Co content decreases the SFE in U2 and facilitates the shearing in the γ matrix. This change also hinders the motion of dislocations and increases the resistance of cross-slip [23]. Therefore, compared to U1, U2 possesses a higher creep resistance and a longer creep life under different experimental conditions.

3 Conclusions

1) The stacking faulting is the main creep mode for the two Ni-based superalloys with different Co contents when $T<725$ °C, while the deformation micro-twinning occurs in two alloys due to the reorder-mediated process when $T\geqslant725$ °C.

2) Moreover, the Co addition tends to lower the SFE, resulting in the dislocation dissociation and shearing process in the γ matrix, which enhances the creep resistance and improves the creep life of the experimental alloys.

References

1 Pollock T M, Argon A S. *Acta Metallurgica et Materialia*[J], 1992, 40(1): 1

2 Mughrabi H, Tetzlaff U. *Advanced Engineering Material*[J], 2000, 2: 319

3 Han G M, Yu J J, Sun Y L *et al. Materials Science and Engineering A*[J]. 2010, 527(21-22): 5383

4 Nembach E, Neite G. *Progress in Material Science*[J], 1985, 29(3): 177

5 Yuan Y, Gu Y, Osada T *et al. Advanced Engineering Material*[J], 2011, 13: 296

6 Yuan Y, Gu Y, Osada T *et al. Scripta Materialia*[J], 2012, 67(2): 137

7 Yuan Y, Gu Y, Osada T *et al. Journal of Microscopy*[J], 2012, 248(1): 34

8 Tian C, Han G, Cui C *et al. Materials & Design*[J], 2015, 88: 123

9 Yuan Y, Gu Y, Cui C *et al. Journal of Materials Research*[J], 2011, 26(22): 2833

10 Ferreira P, Müllner P. *Acta Materialia*[J], 1998, 46: 4479

11 Leverant G, Kear B, Oblak J. *Metallurgical and Materials Transactions B*[J], 1971, 2: 2305

12 Unocic R R, Zhou N, Kovarik L *et al. Acta Materialia*[J], 2011, 59: 7325

13 Bobeck G E, Miner R. *Metallurgical and Materials Transactions A*[J], 1988, 19: 2733

14 Kovarik L, Unocic R R, Li J *et al. Progress in Materials Science* [J], 2009, 54: 839

15 Decamps B, Raujol S, Coujou A *et al. Philosophical Magazine A* [J], 2004, 84: 91

16 Zhang Y H, Chen Q Z, Knowles D M. *Materials Science and Technology*[J], 2001, 17: 1551

17 Viswanathan G, Sarosi P, Henry M *et al. Acta Materialia*[J], 2005, 53: 3041

18 Kamaraj M, Serin K, Kolbe M *et al. Materials Science and Engineering A*[J], 2001, 319: 796
19 Sarosi P M, Viswanathan G B, Mills M J. *Scripta Materialia*[J], 2006, 54: 1157
20 Caron P, Khan T, Veyssiere P. *Philosophical Magazine A*[J], 1988, 57: 589
21 Milligan W W, Antolovich S D. *Metallurgical and Materials Transactions A*[J], 1991, 22: 2309
22 Condat M, Décamps B. *Scripta Materialia*[J], 1987, 21: 607
23 Schumachera G, Darowskia N, Zizak I *et al. Scripta Materialia* [J], 2009, 60: 88

层错能和温度对不同Co含量的镍基高温合金蠕变性能的影响

田成刚[1]，陶稀鹏[2,3]，徐　玲[2]，崔传勇[2]，孙晓峰[2]
(1. 中国航发商用航空发动机有限责任公司，上海 200241)
(2. 中国科学院金属研究所 高温合金部，辽宁 沈阳 110016)
(3. 中国科学技术大学 材料科学与工程学院，辽宁 沈阳 110016)

摘　要：研究了2种不同Co含量的镍基高温合金分别在650 °C/630 MPa，725 °C/630 MPa和760 °C/630 MPa条件下的蠕变变形组织。通过透射电镜分析了温度和层错能对蠕变变形机制的影响。结果表明，对于所选取的高温合金来说，温度的提升可以有效促使蠕变变形机制由层错转变为孪晶。这表明孪晶的形成更大程度上取决于温度。此外，合金Co含量的提升以及层错能的下降都会使层错和孪晶延伸并穿过γ基体和γ'析出相，该方式提升了材料的蠕变抗力以及蠕变寿命。

关键词：高温合金；层错；层错能；孪晶

作者简介：田成刚，男，1987年生，博士，中国航发商用航空发动机有限责任公司，上海 200241，E-mail：562286459@qq.com